THE JOURNAL OF BIOLOGICAL CHEMISTRY VOL. 282, NO. 25, pp. 18510–18520, June 22, 2007

Biochemical and Genetic Studies of UBR3, a Ubiquitin Ligase with a Function in Olfactory and Other Sensory Systems*

Received for publication, March 5, 2007, and in revised form, April 24, 2007 Published, JBC Papers in Press, April 26, 2007, DOI 10.1074/jbc.M701894200

Takafumi Tasaki[‡], Reinhard Sohr[§], Zanxian Xia[¶], Rainer Hellweg[‖], Heide Hörtnagl[§], Alexander Varshavsky[¶], and Yong Tae Kwon[‡1]

From the [‡]Center for Pharmacogenetics and Department of Pharmaceutical Sciences, University of Pittsburgh, Pittsburgh, Pennsylvania 15261, the [§]Institute of Pharmacology and Toxicology, Charité-University Medicine Berlin, Campus Mitte, Dorotheenstrasse 94, D-10117 Berlin, Germany, the [¶]Division of Biology, California Institute of Technology, Pasadena, California 91125, and the [‖]Department of Psychiatry and Psychotherapy, Charité-University Medicine Berlin, Campus Benjamin Franklin, Eschenallee 3, D-14050 Berlin, Germany

Our previous work identified E3 ubiquitin ligases, termed UBR1–UBR7, that contain the ~70-residue UBR box, a motif important for the targeting of N-end rule substrates. In this pathway, specific N-terminal residues of substrates are recognized as degradation signals by UBR box-containing E3s that include UBR1, UBR2, UBR4, and UBR5. The other E3s of this set, UBR3, UBR6, and UBR7, remained uncharacterized. Here we describe the cloning and analyses of mouse UBR3. The similarities of UBR3 to the UBR1 and UBR2 E3s of the N-end rule pathway include the RING and UBR domains. We show that HR6A and HR6B, the E2 enzymes that bind to UBR1 and UBR2, also interact with UBR3. However, in contrast to UBR1 and UBR2, UBR3 does not recognize N-end rule substrates. We also constructed UBR3-lacking mouse strains. In the 129SvImJ background, *UBR3*$^{-/-}$ mice died during embryogenesis, whereas the C57BL/6 background *UBR3*$^{-/-}$ mice exhibited neonatal lethality and suckling impairment that could be partially rescued by litter size reduction. The adult *UBR3*$^{-/-}$ mice had female-specific behavioral anosmia. Cells of the olfactory pathway were found to express β-galactosidase (LacZ) that marked the deletion/disruption *UBR3*$^{-}$ allele. The *UBR3*-specific LacZ expression was also prominent in cells of the touch, vision, hearing, and taste systems, suggesting a regulatory role of UBR3 in sensory pathways, including olfaction. By analogy with functions of the UBR domain in the N-end rule pathway, we propose that the UBR box of UBR3 may recognize small compounds that modulate the targeting, by this E3, of its currently unknown substrates.

A protein substrate of the ubiquitin (Ub)[2]-proteasome system, which controls the levels of many intracellular proteins, is conjugated to Ub through the action of E1, E2, and E3 enzymes (1–4). The selectivity of ubiquitylation is mediated largely by E3, which recognizes a substrate's degradation signal (degron) (5–8). The E3 Ub ligases are an exceptionally large family, with more than 500 distinct E3s in a mammal (9, 10). The term "Ub ligase" denotes either an E2–E3 holoenzyme or its E3 component. A ubiquitylated protein bears a covalently linked poly-Ub chain and is targeted for processive degradation by the 26 S proteasome (11). Ub has other functions as well, including non-proteolytic ones (12, 13). An essential determinant of one class of degrons, called N-degrons, is a substrate's destabilizing N-terminal residue. The set of destabilizing residues in a given cell type yields a rule, called the N-end rule, which relates the *in vivo* half-life of a protein to the identity of its N-terminal residue (Fig. 1*A*) (4, 14–19). In eukaryotes, the N-degron consists of three determinants: a destabilizing N-terminal residue of a protein substrate, its internal Lys residue(s) (the site of formation of a poly-Ub chain), and a conformationally flexible region(s) in the vicinity of these determinants (5, 7, 15, 20, 21).

The N-end rule has a hierarchic structure in that some of the destabilizing N-terminal residues (Arg, Lys, His, Phe, Leu, Trp, Tyr, and Ile) are recognized directly by E3 Ub ligases of the N-end rule pathway, called N-recognins, whereas the other destabilizing N-terminal residues (Asn, Gln, Asp, Glu, and Cys) must be modified *in vivo*, enzymatically or otherwise, for their subsequent (indirect) recognition by these E3s (Fig. 1*A*) (18, 19, 22–25). The functions of the N-end rule pathway include its roles in the control of signaling by nitric oxide and G protein-coupled receptors (GPCRs), the regulation of peptide import, the fidelity of chromosome segregation, the apoptosis, meiosis, cardiovascular development, neurogenesis, and pancreatic functions, and leaf senescence in plants (16, 18, 24–32).

The N-end rule pathway of the yeast *Saccharomyces cerevisiae* is mediated by a single N-recognin, the Ub ligase UBR1 (33), whereas at least four N-recognins, including UBR1, medi-

* This work was supported by National Institutes of Health Grants GM69482, GM074000, and HL083365 (to Y. T. K.) and GM31530 and DK39520 (to A. V.) and also by the grants from the American Heart Association (to Y. T. K.), the Ellison Medical Foundation (to A. V.), and the Charité-Universitätsmedizin Berlin (to R. S., R. H., and H. H.). The costs of publication of this article were defrayed in part by the payment of page charges. This article must therefore be hereby marked "*advertisement*" in accordance with 18 U.S.C. Section 1734 solely to indicate this fact.

The nucleotide sequence(s) reported in this paper has been submitted to the GenBank™/EBI Data Bank with accession number(s) DQ924536.

[1] To whom correspondence should be addressed: Center for Pharmacogenetics and Dept. of Pharmaceutical Sciences, University of Pittsburgh, 3501 Terrace St., Pittsburgh, PA 15261. Tel.: 412-383-7994; Fax: 412-648-1664; E-mail: yok5@pitt.edu.

[2] The abbreviations used are: Ub, ubiquitin; E1, ubiquitin-activating enzyme; E2, ubiquitin carrier protein; E3, ubiquitin-protein isopeptide ligase; GPCR, G protein-coupled receptor; GST, glutathione *S*-transferase; MOE, main olfactory epithelium; VNO, vomeronasal organ; OB, olfactory bulb; OC, olfactory cortex; HPLC, high performance liquid chromatography; ES, embryonic stem.

ate this pathway in mammals (16, 17, 31, 34). Our recent study (17) identified a family of mammalian E3 Ub ligases that share a characteristic zinc finger-like ~70-residue domain termed the UBR box. The mouse genome encodes at least seven UBR box-containing proteins, termed UBR1–UBR7, which vary both in size (from 50 to 570 kDa) and in containing or lacking other E3-characteristic domains, such as HECT, RING, PHD, or F-box (Fig. 1*B*) (17). UBR1 and UBR2 of this set, the highly homologous (47% identical) 200-kDa E3s, are the known N-recognins of the mouse N-end rule pathway (16, 34).

In the *S. cerevisiae* RING-type UBR1 Ub ligase and also (by inference) in its mammalian homologs UBR1 and UBR2, the UBR box and nearby regions mediate the recognition of N-degrons (*i.e.* the binding of N-recognin to a primary destabilizing N-terminal residue (Arg, Lys, His, Phe, Leu, Trp, Tyr, or Ile) of a polypeptide) (16, 33). *S. cerevisiae* UBR1 recognizes type-1 (basic) destabilizing N-terminal residues Arg, Lys, and His through a binding site that resides at least in part in the UBR box. UBR1 recognizes type-2 (bulky hydrophobic) N-terminal residues Phe, Leu, Trp, Tyr, and Ile through a nearby but genetically distinguishable domain that includes the UBR box and a proximal downstream region (see Refs. 17, 33, and 35 and references therein). *S. cerevisiae* UBR1 contains yet another (third) substrate-binding site. Its activity is allosterically controlled by occupancy states of the other two (type-1 and type-2) binding sites of UBR1. The third substrate-binding site targets the transcriptional repressor CUP9, through an internal degron near the C terminus of CUP9 (26, 33). Since mouse UBR1 and UBR2 are homologs of *S. cerevisiae* UBR1 (16, 36), one would expect these mammalian Ub ligases to also contain analogous (third) substrate-binding sites (Fig. 1*A*). Indeed, mouse UBR1 was shown to target c-FOS, a component of the AP-1 transcription factor, for ubiquitylation and subsequent degradation through a conditional (regulated by phosphorylation) degron near the N terminus of c-FOS (37). Several other UBR box-containing proteins, such as UBR4 (PUSHOVER/BIG) and UBR5 (EDD/hHYD), are also, operationally, N-recognins whose substrate specificities include the ability to recognize primary destabilizing N-terminal residues (Fig. 1*A*) (17).

We have previously characterized mammalian UBR1, UBR2, UBR4, and UBR5 as Ub ligases of the N-end rule pathway that recognize destabilizing N-terminal residues (16, 17, 34, 36). In the present study, we cloned and characterized mouse UBR3, a protein of unknown function that contains both the UBR box and the RING domain. Our findings show that UBR1, UBR2, and UBR3 are structurally related members of the RING-UBR subfamily of UBR-box E3s that interact (and function together) with the E2 enzymes HR6A and HR6B. We also constructed and characterized mouse strains lacking UBR3 and describe several lines of evidence suggesting that one function of UBR3 involves the regulation of sensory pathways, including olfaction.

EXPERIMENTAL PROCEDURES

Cloning of the UBR3 cDNA—A 412-bp cDNA fragment that encompassed a 3′-proximal region of the *UBR3* ORF (see "Results") was used as a probe to screen a λEXlox-based embryonic day 10 (E10) mouse embryo cDNA library (Novagen, Madison, WI), yielding a 2.5-kb *UBR3* cDNA fragment. This fragment was employed as a probe in a second screen, using a λgt10-based mouse cDNA library from MEL-C19 cells (Clontech) and yielding in a 1-kb fragment. Two subsequent screenings yielded 2-kb and 1.5-kb fragments. To isolate the 5′ region of *UBR3* cDNA, 5′-rapid amplification of cDNA ends PCR was performed with poly(A)$^+$ RNA from mouse liver or skeletal muscle. The resulting set of overlapping cDNA fragments were joined to produce full-length *UBR3* cDNAs encoding two splicing-derived isoforms.

Construction of UBR3$^{-/-}$ Mouse Strains—The mouse *UBR3* gene was isolated by screening a bacterial artificial chromosome (BAC) DNA library (Genome Systems, St. Louis, MO) from 129SvJ mouse embryonic stem (ES) cells by using a *UBR3*-specific cDNA probe (nucleotides 385–1,886). The exon/intron organization of the first ~30 kb of UBR3 was determined using exon-specific PCR primers to amplify genomic DNA fragments flanked by exons as previously described (34). The targeting vector was constructed using standard techniques, linearized with KpnI, and electroporated into CJ7 ES cells, followed by standard procedures for selection and identification of correctly targeted *UBR3*$^{+/-}$ ES cell colonies by using PCR and Southern hybridization (16, 22, 24, 34, 38). The resulting *UBR3*$^{+/-}$ ES cell clones (6 of 960 ES cell clones analyzed) were further selected for apparently normal karyotypes. Four independently produced *UBR3*$^{+/-}$ ES cell clones were injected into C57/BL6J blastocysts to generate chimeric mice. In two of these mice, the mutant (*UBR3*$^{-}$) allele was transmitted to the germ line. Northern and Southern hybridizations and PCR-mediated genotyping were carried out as described (34).

GST Pull-down Assays—Glutathione *S*-transferase (GST) pull-down assays were carried out as described (16). N-terminally FLAG-tagged mouse ^{f}UBR1, ^{f}UBR2, and ^{f}UBR3 and *S. cerevisiae* ^{f}UBR1 (sc-^{f}UBR1) were expressed in *S. cerevisiae* SC295 (*MATa, GAL4 GAL80 ura3-52, leu2-3,112 reg1-501 gal1 pep4-3*) from the P_{ADH1} promoter in a high copy vector. *X*-SCC1-GST fusions (where *X* represents Met, Arg, or Leu) were produced using the IMPACT (intein-mediated purification with an affinity chitin-binding tag) system (New England Biolabs, Ipswich, MA) as previously described (16). N-terminal residues of the test proteins were verified by Edman sequencing of purified *X*-SCC1-GST fusions. GST fusions to mouse HR6A and HR6B (GST-HR6A and GST-HR6B) were expressed in *Escherichia coli* BL21(DE3) and purified as described (16). The purified *X*-SCC1-GST (2 μg) in 250 μl of the loading buffer (137 mM NaCl, 2.7 mM KCl, 4.3 mM Na_2HPO_4, 1.4 mM KH_2PO_4, 10% glycerol, and 1% Triton X-100, pH 7.4) was incubated with 15 μl of glutathione-Sepharose beads (Amersham Biosciences) for 1 h at 4 °C. The beads were washed once with the loading buffer and twice with the binding buffer (10% glycerol, 0.1% Nonidet P-40, 0.2 M KCl, 1 mM dithiothreitol, and 50 mM HEPES, pH 7.5). The diluted yeast extracts (250 μl) containing E3s in binding buffer containing the protease inhibitor tablet (Roche Applied Science) were added into the washed beads. The bound proteins were eluted, fractionated by SDS-PAGE, and immunoblotted with anti-FLAG antibody. The *5% input lanes* (see Fig. 2) refer to a directly loaded sample of the yeast extract that

corresponded to 5% of the extract amount used in GST pull-down assays.

X-Peptide Pull-down Assay—*X*-Peptides (*X*-Ile-Phe-Ser-Thr-Asp-Thr-Gly-Pro-Gly-Gly-Cys, where *X* represents Arg, Phe, Gly, Ser, Thr, Ala, Asp, or Met), where residues 2–9 were derived from residues 2–9 of Sindbis virus polymerase nsP4, were synthesized as described (17). *S. cerevisiae* extract expressing mouse ^{f}UBR1, ^{f}UBR2, or ^{f}UBR3 was diluted by the lysis buffer (10% glycerol, 0.1% Nonidet P-40, 0.2 M KCl, 1 mM dithiothreitol, and 50 mM HEPES, pH 7.5) to 1.2 mg/ml of total protein and thereafter incubated with or without an added dipeptide for 15 min on ice to prevent proteolytic degradation of peptide substrates. A sample (0.3 ml) was then transferred to a new tube containing 5 μl (packed volume) of a carrier-linked 12-mer peptide, followed by gentle mixing, through rotation of the tube, for 1 h at 4 °C. The beads were pelleted by a brief centrifugation and then washed three times, for 2 min each, with the lysis buffer. The beads were then suspended in 20 μl of SDS-PAGE loading buffer and heated at 95 °C for 5 min, followed by a brief spin in a microcentrifuge, SDS-8% PAGE of the supernatant, and detection of ^{f}UBR1, ^{f}UBR2, or ^{f}UBR3 by immunoblotting with anti-FLAG M2 antibody.

Antibody to Mouse UBR3—An affinity-purified polyclonal rabbit antibody to mouse UBR3 was produced using standard methods (34, 38, 39), using purified GST-UBR3-(182–598) fusion as an antigen. This antibody was employed to detect endogenous UBR3 through a combination of immunoprecipitation and immunoblotting (see Fig. 3*D* and "Results").

LacZ Staining, Immunohistochemistry, and Northern Hybridization—LacZ staining (using 5-bromo-4-chloro-3-indolyl-β-D-galactopyranoside) and Northern hybridization (with a *UBR3*-specific ^{32}P-labeled cDNA probe) were carried out as described (24). LacZ-stained embryos were postfixed, photographed, and sectioned after embedding in paraffin. Alternatively, the tissues were frozen in OCT medium after fixation, cryosectioned, and stained for LacZ on the slides. For immunohistochemistry, specific tissues were isolated, fixed in 4% formaldehyde, treated with 70% ethanol, dehydrated, and embedded in paraffin wax as described (16), followed by sectioning and staining with hematoxylin/eosin or an antibody. For Northern hybridization, a mouse adult tissue blot (Seegene, Seoul, Korea) containing total RNAs isolated from the brain, heart, lung, liver, spleen, kidney, stomach, small intestine, skeletal muscle, thymus, testis, uterus of nonpregnant female, and E17.5 placenta was hybridized with ^{32}P-labeled cDNA fragments of mouse *UBR3* or human β-actin. Northern analyses were also done with total RNAs from *UBR3*$^{-/-}$ brains and hearts *versus* their wild-type counterparts.

Assays for Neurotransmitters, Amino Acids, and Neurotrophins—Individual brains for each *UBR3* genotype (+/+, +/−, and −/−) at the stages of E18 and postnatal day 1 (P1) were collected (6–8 brains of each genotype) to measure neurotransmitters and related compounds as described (40). The levels of monoamines (noradrenaline, dopamine, and serotonin) and their metabolites were determined using high performance liquid chromatography (HPLC) with electrochemical detection. Amino acids were measured using HPLC and fluorescence spectroscopy (41). The levels of nerve growth factor and brain-derived neurotrophic factor in the brains were determined by enzyme-linked immunoassay (42).

Odor-based Behavioral Tests—Odorant discrimination tests were performed largely as described (43) with minor modifications. *UBR3*$^{-/-}$ mice (7–17 weeks old) with littermate controls (+/+ and *UBR3*$^{+/-}$) were individually housed in filter-topped cages 2 days before the test. On the third day, the test mouse was relocated to a designated area away from other mice and was left there for 30 min to allow accommodation to the environment. Pretraining sessions and odorant tests with mice are described under "Results." Odorant solutions (50 μM) were made freshly in deionized water (for isoamyl acetate and ethyl vanillin) or mineral oil (for geraniol and citral). One experimenter performed the entire set of odorant tests without knowing the genotypes of mice being tested.

RESULTS

Cloning of Mouse cDNAs Encoding UBR3—Data base search using UBR1 and UBR2 sequences as probes brought forth a 388-bp cDNA fragment (GenBank^{TM} accession number W83893) encoding a partial open reading frame that exhibits a weak but significant homology to C-terminal regions of UBR1 and UBR2. By employing cDNA library screening and 5′-rapid amplification of cDNA ends PCR, we cloned the ~8-kb full-length mouse cDNA, yielding nine overlapping cDNA fragments that represented two isoforms of a ~213-kDa protein named UBR3. The predicted mouse *UBR3* cDNA isoforms, encoding the proteins of 1,889 and 1,893 residues, respectively, contained distinct exon/intron boundaries, indicating alternative RNA splicing (data not shown). Reverse transcription-PCR analysis detected comparable mRNA levels of UBR3 isoforms in the liver and skeletal muscle (data not shown). Northern hybridization indicated that the two *UBR3* mRNAs, of ~8 and ~6.5 kb, were expressed in a broad range of tissues, with higher levels in the brain and skeletal muscle (Fig. 1*D*). UBR3 exhibited a low but significant sequence similarity (22% identity) to the 200-kDa mouse UBR1 and UBR2, which are 47% identical (Fig. 1*C*). Significantly, UBR3 contained all of the domains (the UBR box, the WxRNG domain, the RING-H2 finger, and the autoinhibitory domain) that have been identified in UBR1 and UBR2 (Fig. 1*C*). Thus, operationally, UBR1, UBR2, and UBR3 comprise a distinct RING-UBR subfamily of UBR Ub ligases.

UBR3 Binds to E2 Ub-conjugating Enzymes HR6A and HR6B—We have previously shown that either of the E2 Ub-conjugating enzymes HR6A and HR6B supports the UBR1-mediated degradation of N-end rule substrates (34) and that mouse UBR1 and UBR2 bind to HR6B (16). Mouse HR6A and HR6B are 95% identical and are functional counterparts of the *S. cerevisiae* E2 enzyme RAD6/UBC2 whose multiple functions include the N-end rule pathway, where RAD6 is a part of the UBR1-RAD6 Ub ligase (44, 45). To determine whether mouse UBR3 binds to HR6A and HR6B, we expressed the N-terminally FLAG-tagged mouse ^{f}UBR3 and ^{f}UBR1 in *S. cerevisiae*. Purified GST-HR6A or GST-HR6B fusion proteins were bound to glutathione-conjugated beads, and GST pull-down assays were carried out with yeast extracts expressing ^{f}UBR1 or ^{f}UBR3. Both ^{f}UBR3 and ^{f}UBR1 bound to GST-HR6A and GST-HR6B but not to *S. cerevisiae*-derived GST-RAD6 (negative control) (Fig. 2, *A* and *B*).

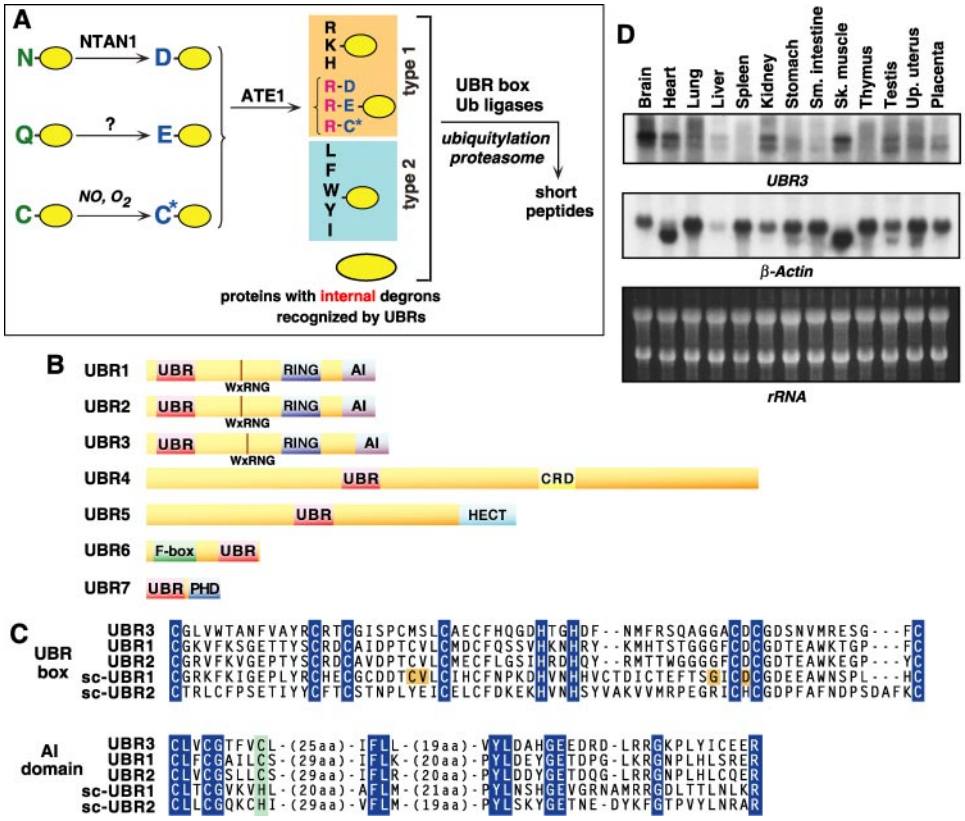

FIGURE 1. **The N-end rule pathway and the UBR3 ubiquitin ligase.** *A*, the mammalian N-end rule pathway. N-terminal residues are indicated by *single-letter abbreviations* for amino acids. The *yellow ovals* denote the rest of a protein substrate. *C**, oxidized N-terminal Cys, either Cys-sulfinic acid ($CysO_2(H)$) or Cys-sulfonic acid ($CysO_3(H)$), produced in reactions mediated by nitric oxide (*NO*) and oxygen (O_2) or its derivatives, with subsequent arginylation of oxidized Cys by the *ATE1*-encoded isoforms of Arg-tRNA-protein transferase (see Introduction). Through their other substrate-binding sites, these E3 enzymes also recognize internal (non-N-terminal) degrons in other substrates of the N-end rule pathway, denoted by a *larger oval*. *B*, locations of the UBR boxes and several other domains characteristic, in particular, of E3 Ub ligases (17). *C*, sequence alignment of the UBR boxes and autoinhibitory (*AI*) domains of mouse UBR1–UBR3, and in *S. cerevisiae* UBR1 and UBR2. The residue numbers of UBR3 corresponding to its (shown) UBR and AI domains are 120–184 and 1,780–1,862, respectively. *Yellow shading* highlights the residues of *S. cerevisiae* UBR1 that are essential for the UBR1-dependent degradation of type-1 N-end rule substrates (see Ref. 17 and references therein). *D*, Northern blot analysis of *UBR3* and β-actin using different mouse adult tissues. Total RNA (20 μg) was loaded in each *lane*, and the ethidium bromide-stained ribosomal RNAs (*rRNA*) were shown as a loading control (*bottom*). Data for β-actin and ribosomal RNAs have been presented as controls for Northern blot analysis of *UBR4* (17).

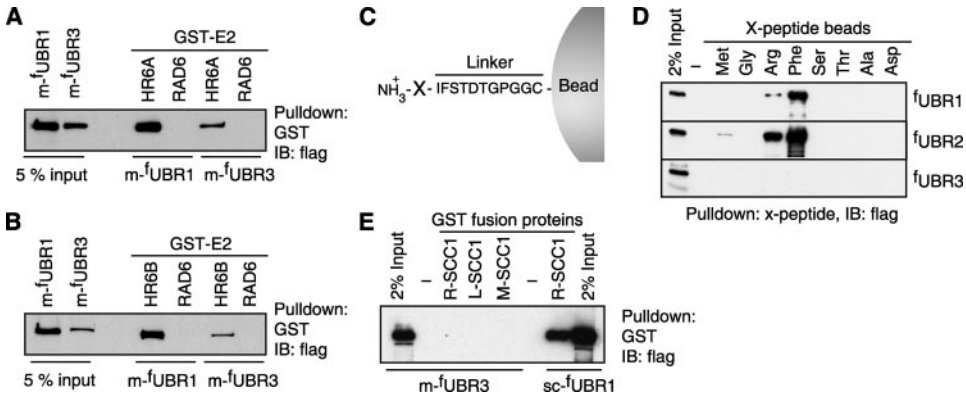

FIGURE 2. **Analyses of interactions of UBR3 with E2 Ub-conjugating enzymes and N-terminal residues of peptide probes.** *A*, m-UBR3 binds to the HR6A E2 enzyme. Extracts (1.5 mg of protein) from *S. cerevisiae* expressing FLAG-tagged mouse UBR3 (^{f}UBR3) were incubated with glutathione-Sepharose beads preloaded with GST-HR6A (mouse HR6A) or GST-RAD6 (yeast RAD6). The bound proteins were eluted, fractionated by SDS-7.5% PAGE, and immunoblotted (*IB*) with anti-FLAG antibody. *5% input*, 5% of the yeast extract used in a single GST assay. *B*, same as in *A* but with GST-HR6B. *C*, bead-conjugated *X*-peptides bearing different N-terminal residues. *D*, *X*-peptide pull-down assay with mouse UBR1, UBR2, and UBR3. Extracts from *S. cerevisiae* expressing ^{f}UBR1, ^{f}UBR2, or ^{f}UBR3 were incubated with an *X*-peptide on beads, followed by pelleting of the beads, washing, SDS-PAGE, and anti-FLAG immunoblotting. *E*, GST pull-down of *S. cerevisiae* UBR1 (sc-^{f}UBR1) and mouse UBR3 with reporter proteins *X*-SCC1-GST (where *X* represents Met, Arg, or Leu).

Together with earlier findings with mouse UBR1 and UBR2 (16, 34), these results (Fig. 2, *A* and *B*) suggest that HR6A and HR6B are E2s that form the holoenzyme Ub ligases with, in particular, E3s of the RING-UBR subfamily. The latter consists, at present, of UBR1, UBR2, and UBR3.

UBR3 Does Not Bind to Known N-end Rule Substrates of UBR1 and UBR2—The *X*-peptide pull-down assay that we developed previously (17) was used to determine whether UBR3 can recognize destabilizing N-terminal residues that are known to be bound by UBR1 and UBR2 (Fig. 2*C*). An *S. cerevisiae* extract expressing ^{f}UBR1, ^{f}UBR2, or ^{f}UBR3 was incubated with an immobilized 12-mer *X*-peptide (*X*-Ile-Phe-Ser-Thr-Asp-Thr-Gly-Pro-Gly-Gly-Cys, where *X* represents Arg (type-1 primary destabilizing residue), Phe (type-2 primary destabilizing residue), Asp (secondary destabilizing residue), Met, Gly, Ser, Thr, or Ala), followed by a pull-down assay and anti-FLAG immunoblotting. Consistent with earlier results (17), ^{f}UBR1 and ^{f}UBR2 bound to *X*-peptides bearing either type-1 or type-2 destabilizing N-terminal residues but not to other N-terminal residues (Fig. 2*D*). In contrast, ^{f}UBR3 did not bind to any of the tested *X*-peptides (Fig. 2*D*). To verify this finding, we employed a different binding assay, with *X*-SCC1-GST fusions (where *X* represents Arg (type-1 destabilizing residue), Leu (type-2 destabilizing residue), or Met (stabilizing residue)). The SCC1 moiety of these fusions is a 33-kDa separase-produced C-terminal fragment of the *S. cerevisiae* cohesin subunit SCC1 that bears N-terminal Arg and is rapidly degraded by the N-end rule pathway (16, 27). As expected, sc-^{f}UBR1 bound to Arg-SCC1 but not to Met-SCC1. However, ^{f}UBR3 did not interact with any of these substrates (Fig. 2*E*), consistent with both the present *X*-peptide data (Fig. 2*D*) and the analogous earlier assays with mouse tissue extracts that identified UBR1, UBR2, UBR4, and UBR5 but

not UBR3 (17) (data not shown). We conclude that UBR3 does not bind to known substrates of the N-end rule pathway.

The pattern of E2–E3 interactions in the mammalian RING-UBR subfamily is analogous to the disposition in *S. cerevisiae*, where RAD6, a homolog of HR6A and HR6B, functions as a common E2 for the yeast RING-UBR subfamily, which consists of sc-UBR1 (the sole E3 of the *S. cerevisiae* N-end rule pathway) (15) and sc-UBR2, which does not bind to N-end rule substrates (46). It remains to be determined whether mammalian UBR3 is functionally analogous to sc-UBR2.

UBR3 Knock-out in Mice Results in Strain-dependent Phenotypes—To address the physiological functions of UBR3, we constructed *UBR3*$^{-/-}$ mouse strains. BAC clones encoding mouse *UBR3* were isolated from a strain 129-derived SvJ BAC library. Data base analyses indicated that *UBR3* encompasses ~130 kb of mouse chromosome 2 and ~260 kb of human chromosome 2. Using restriction mapping and sequencing, we determined the structure of a ~30-kb genomic fragment spanning the 5′ upstream region and exons 1–5 of mouse *UBR3*. In the *UBR3* targeting vector, a region spanning exon 1 (encoding most the UBR box) and its flanking intron were replaced with *nlsLacZ-neo* that encodes *E. coli lacZ* (β-galactosidase) fused to a nuclear localization signal, followed by the floxed (flanked by the *loxP* sites) *PGK/Neo* cassette. In the resulting *UBR3*$^{-}$ deletion/disruption allele, the *nlsLacZ* mRNA is produced from the endogenous *UBR3* promoter (Fig. 3*A*). Mouse chimeras carrying the desired *UBR3*$^{-}$ (*UBR3*^{nlsLacZ}) allele were produced using standard ES cell-based methods (16, 22, 24, 34). These mice were crossed with either C57BL/6J (denoted as B6) or 129SvImJ (denoted as 129S) wild-type females, yielding F1 *UBR3*$^{+/-}$ offspring in either mixed (B6/129S) or inbred (129S) backgrounds. The deletion/disruption *UBR3*$^{-}$ allele was confirmed by Southern analysis (Fig. 3*B*), and the absence of *UBR3* mRNA in *UBR3*$^{-/-}$ mice was confirmed by Northern analysis (Fig. 3*C*). The purified GST-UBR3-(182–598) fusion protein was used as an antigen to produce a polyclonal, affinity-purified anti-UBR3 antibody (see "Experimental Procedures"). Anti-UBR3 immunoprecipitation-immunoblotting with mouse tissue extracts confirmed the absence of UBR3 in *UBR3*$^{-/-}$ mice (Fig. 3*D*).

UBR3$^{-/-}$ mice in the mixed (B6/129S) background were born at a frequency slightly lower than the expected Mendelian frequency (Table 1). They were fertile and apparently normal, indicating that UBR3 is not essential for viability and fertility in this genetic background. In contrast, no *UBR3*$^{-/-}$ mice in the inbred (129S) background were retrieved from 207 adult mice and 78 embryos (from E3.5 to E16.5) that were produced from heterozygous intercrosses, suggesting that *UBR3* knock-out in this background causes lethality in early embryogenesis. We therefore wished to analyze the phenotypes of *UBR3*$^{-/-}$ mice in a C57BL/6J (B6)-enriched genetic background. B6-enriched *UBR3*$^{+/-}$ mice were produced through backcrosses to wild-type B6 females for 8–12 generations (N8–N12) over a period of ~3 years. Unexpectedly, these (B6-enriched) *UBR3*$^{-/-}$ mice exhibited neonatal lethality.

Impaired Suckling and Neonatal Death of B6 Background UBR3$^{-/-}$ *Mice*—B6 background-enriched *UBR3*$^{-/-}$ embryos were apparently normal in growth and other developmental features. At birth, their body weight (1.30 ± 0.04 g; $n = 15$) was ~10% lower compared with +/+ pups (1.46 g ± 0.05; $n = 10$). Despite the growth retardation, *UBR3*$^{-/-}$ neonates appeared normal in body color, breathing behavior, touch response,

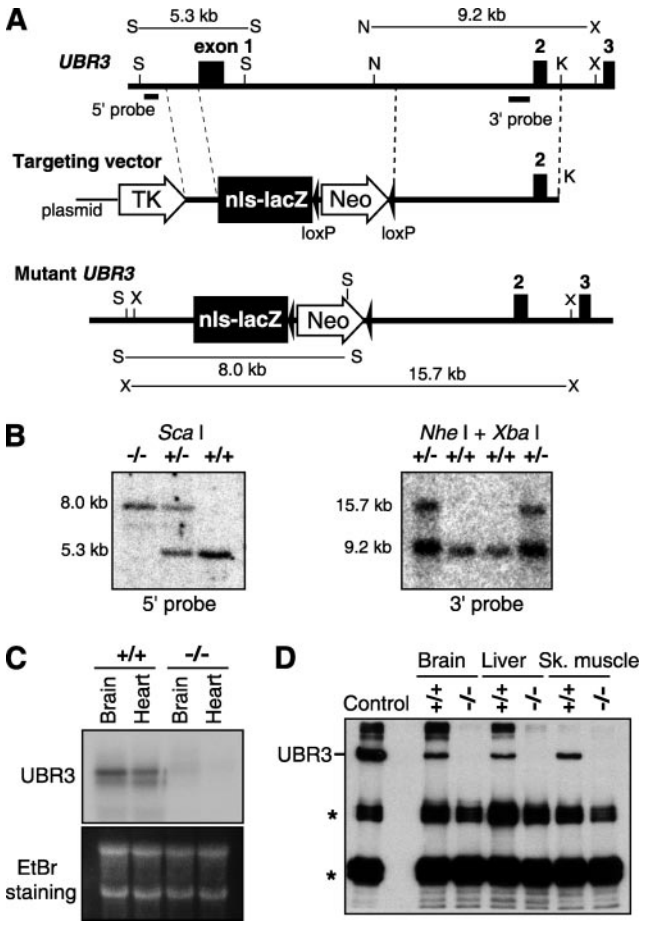

FIGURE 3. **Construction of *UBR3*$^{-/-}$ mouse strains.** *A*, a map of the ~24-kb 5′-proximal region of the ~130-kb *UBR3* gene, the targeting vector, and the deletion/disruption *UBR3*$^{-/-}$ allele. Exons are denoted by *vertical rectangles*. *Thick* and *thin lines* describe, respectively, the mouse and bacterial (plasmid-derived) DNA sequences. Selection markers (thymidine kinase (*TK*) and neomycin (*Neo*) genes), the *nls-lacZ* cassette, and the *loxP* sites are shown as *open arrows*, a *solid box*, and *solid arrowheads*, respectively. Southern blot probes are indicated by *solid horizontal bars*. Restriction sites were as follows: ScaI (*S*), NheI (*N*), XbaI (*X*); and KpnI (*K*). *B*, Southern analysis of ScaI-cut and NheI/XbaI-cut mouse tail DNAs from +/+, *UBR3*$^{+/-}$, and *UBR3*$^{-/-}$ mice, hybridized with 0.2-kb (*5′-probe*) and 0.6-kb (*3′-probe*) fragments of *UBR3*. *C*, Northern analysis of m-*UBR3* expression, using total RNA from the brains and hearts of +/+ and *UBR3*$^{-/-}$ mice. Ethidium bromide-stained ribosomal RNAs, a loading control, are also shown. *D*, immunoprecipitation-immunoblotting detection of UBR3 in extracts from the brain, liver, and skeletal muscle (*Sk. muscle*) of +/+ and *UBR3*$^{-/-}$ mice. The *Control lane* denotes a sample of extract from *S. cerevisiae* expressing ^{f}UBR3. *, bands of IgG.

TABLE 1

Genotypes of 3-week-old offspring from *UBR3*$^{+/-}$ intercrosses in different genetic backgrounds

Genotype	Number of mice of background		
	129S/B6 (mixed)	B6 (enriched)	129S (coisogenic)
+/+	106	42	54
+/−	178	70	153
−/−	70	**15**[a]	**0**
Total	354	127	207
Average litter size	8	7.9	5.9

[a] Numbers in boldface type refer to apparently underrepresented genotypes, in comparison with +/+.

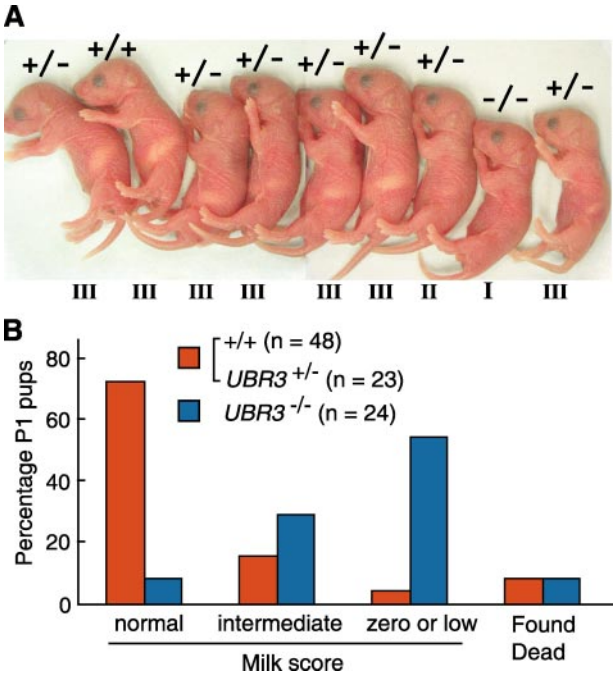

FIGURE 4. **Impaired suckling in *UBR3*$^{-/-}$ neonatal pups.** *A*, appearance of a single litter of neonatal pups from a cross between *UBR3*$^{+/-}$ parents, showing the absence (or low amount) of milk in the stomach of a *UBR3*$^{-/-}$ pup. The relative amounts of milk in the stomachs were scored visually as "zero or low" (*I*), "intermediate" (*II*), and "normal" (*III*). *B*, percentages of *UBR3*$^{-/-}$, *UBR3*$^{+/-}$, and +/+ neonatal pups that scored as described above, with 100% representing all pups of a given genotype. The numbers of scored pups with these genotypes are indicated as well (*n*). These comparisons involved, in particular, 24 *UBR3*$^{-/-}$ pups.

righting, and vocalization, indicating that they were not severely impaired in cardiovascular and respiratory systems, motor coordination, and related functions. Notably, however, ~60% of *UBR3*$^{-/-}$ neonatal pups exhibited impaired milk suckling, as determined by the presence and amounts of milk in the stomachs (Fig. 4). Although *UBR3*$^{-/-}$ pups were present in the nest together with littermates and moved their mouths apparently normally, the affected *UBR3*$^{-/-}$ pups became weak, exhibited dehydration, and usually died within 2 days after birth. Dead *UBR3*$^{-/-}$ pups did not exhibit significant anatomical abnormalities in the palate, mouth, and esophagus in comparison with wild-type pups or surviving *UBR3*$^{-/-}$ pups. Both *UBR3*$^{+/-}$ and *UBR3*$^{-/-}$ mothers appeared to nurture their pups normally, showing standard crouching, retrieving, and stimulating responses toward all newborns. In summary, the absence of UBR3, in a B6-enriched background, results in neonatal lethality associated with suckling defects, a phenotype we began to investigate through experiments described below.

Olfaction is crucial for suckling in neonatal mice in that pheromones and other olfactants from the nipple are the main sensory cues used in the nipple's localization by pups. Tactile sensation is also important for suckling behavior, because a rooting reflex is activated, in part, by touching a nipple, a step that initiates the rhythmic mouth movement and swallowing. Indeed, impaired suckling behavior is a typical abnormal phenotype in neonates with mutations in genes required for olfaction or tactile sensation (47–50). Mutant neonates impaired in olfaction or tactile sensation can be partially rescued if the litter size is reduced (48). To examine this possibility with *UBR3*$^{-/-}$ mice, most of the apparently normal (with milk in their stomachs) pups at P1 were removed from three litters ($n = 29$ pups), so that the litters (each of them reduced to three or four pups) contained 1–4 suckling-impaired pups per litter. Of the seven suckling-impaired pups in three reduced size litters, four pups (three *UBR3*$^{-/-}$ and one *UBR3*$^{+/-}$) survived until adulthood, whereas one *UBR3*$^{-/-}$ pup was found dead, and two were cannibalized. The surviving *UBR3*$^{-/-}$ pups grew to adulthood without significant growth retardation and were fertile, with normal mating behavior. These results suggest that litter size reduction, and thereby a reduced competition for lactating nipples, could partially rescue neonatal *UBR3*$^{-/-}$ pups and that B6 background *UBR3*$^{-/-}$ neonates die of starvation rather than developmental failure.

Expression of LacZ/UBR3 in Sensory Cells for Olfactory and Tactile Sensation—Given the phenotype of impaired suckling in B6-enriched *UBR3*$^{-/-}$ pups, we employed the *nls-lacZ* reporter to examine the expression patterns of *UBR3* (Fig. 3*A*), with an emphasis on sensory tissues. LacZ expression patterns in various organs did not differ significantly between *UBR3*$^{-/-}$ and *UBR3*$^{+/-}$ mice, indicating that *UBR3* knock-out did not cause major developmental abnormalities. Odorants and pheromones (*i.e.* the odorants of conspecific origin) are detected primarily by the main olfactory epithelium (MOE) and the vomeronasal organ (VNO), respectively (51, 52). The binding of olfactants to G protein-coupled olfactory receptors (53) on the surfaces of olfactory sensory neurons in MOE initiates signaling cascades that involve specific receptor-coupled G proteins and their transient activation by receptor-bound odorants. This activation transduces and amplifies the initial signal through production of cyclic AMP and phosphoinositide derivatives, activating specific ion channels in an olfactory neuron. The resulting changes in membrane potential give rise to action potentials that propagate from olfactory neurons to a glomerular region of the olfactory bulb (OB), where synaptic connections with mitral cells convey the resulting (processed) signals to olfactory cortex (OC) (52, 54). In contrast, pheromones are detected by specific GPCRs in VNO. The axons of vomeronasal sensory neurons project to mitral cells in glomeruli of the accessory olfactory bulb, relaying the (processed) signals to other regions of the brain (54). *LacZ*-marked *UBR3* was found to be prominently expressed in cells of the olfactory pathway, including the olfactory cell layer of MOE, a mitral neuron cell layer of OB, and a pyramidal cell layer of the piriform cortex of OC (Fig. 5, *A–E*). The expression of *UBR3* was also strong in the vomeronasal sensory epithelium of VNO and the mitral cells of the accessory olfactory bulb (Fig. 5, *F* and *G*). In neonates, tactile stimuli to whiskers and sinus hairs of lips activate primary somatosensory afferent neurons (trigeminal nerve) that innervate vibrissal follicle-sinus complexes (49). *UBR3* was prominently expressed in tactile tissues, including the dorsal root ganglion, trigeminal ganglion, and follicle-sinus complexes (Fig. 6, *A–F*). In follicle-sinus complexes, the *UBR3*-specific LacZ staining was prominent in cells between hair follicle and sinus and also in the region of the rete ridge collar (Fig. 6, *E* and *F*). These results indicated that *UBR3* is prominently expressed in sensory cells involved in olfactory and tactile sensations, both of which are important for normal suckling in neonatal mice.

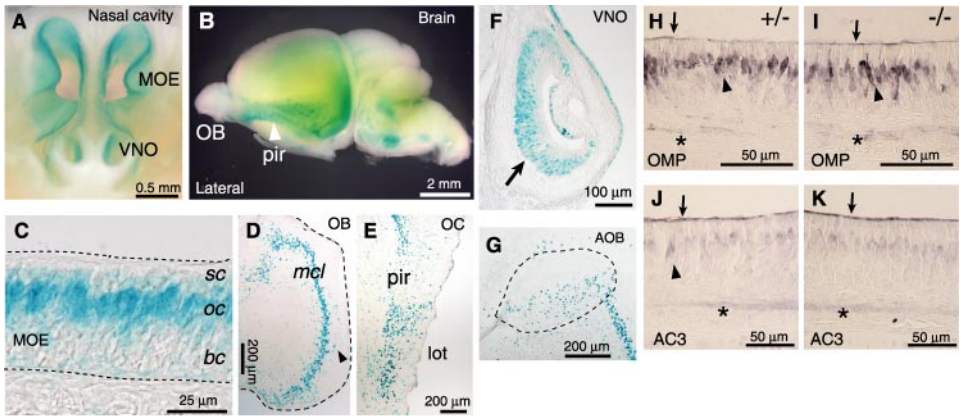

FIGURE 5. **Expression of mouse *UBR3* in the nose and olfaction-relevant brain regions.** *A–G*, staining for the LacZ (βgal)-marked *UBR3*$^{-}$ allele (*UBR3*^{nlsLacZ}) of 1-day-old (P1) *UBR3*$^{-/-}$ pups. *A* and *B*, whole mount LacZ staining of the nasal cavity and brain, showing the expression of *UBR3* in the MOE, VNO, and piriform cortex (*pir*). *C–F*, coronal sections of the nose, with *UBR3* expression specifically in olfactory cells (*oc*) of MOE (*C*), in the mitral cell layer (*mcl*) in periglomerular cells (*arrowhead*) of OB (*D*), in the *pir* region of the olfactory cortex (*OC*) (*E*), and in vomeronasal neurons (*arrow*) of VNO (*F*). *G*, coronal section of the brain, with *UBR3* expression in the accessory olfactory bulb (*AOB*) (*dotted area*). *sc*, support cells; *bc*, basal cells; *lot*, lateral olfactory tract. *H–K*, immunohistochemical detection of the olfactory marker protein (*OMP*) (*H* and *I*) and type III adenylyl cyclase (*AC3*) (*J* and *K*) in *UBR3*$^{+/-}$ (*H* and *J*) and *UBR3*$^{-/-}$ (*I* and *K*) P1 pups. The target-specific staining was significant in cilia (*arrows*), olfactory cells (*arrowheads*), and axon bundles (*asterisks*).

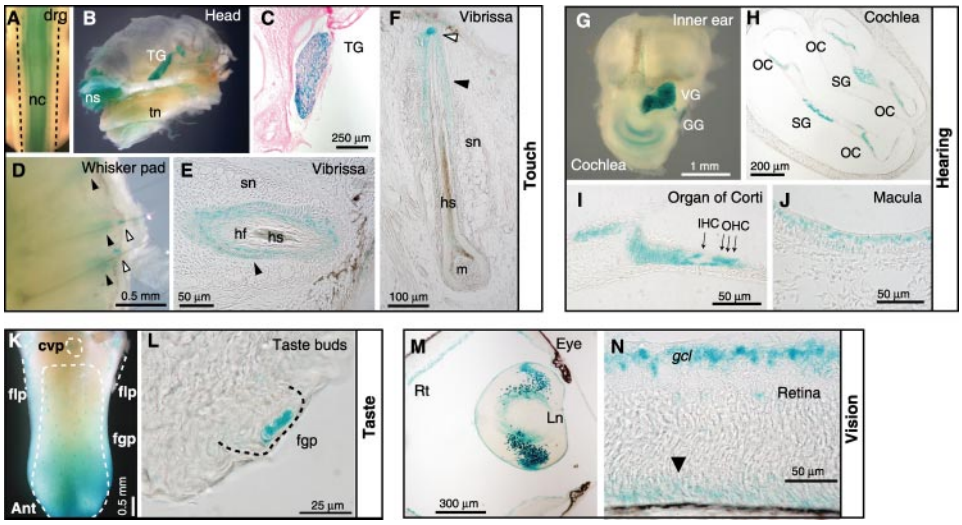

FIGURE 6. **Expression of mouse *UBR3* in tissues relevant to the sensation of touch, hearing, taste, and vision.** *A–F*, expression of *UBR3*, as determined by LacZ staining (see the legend to Fig. 5), in tissues mediating the sensation of touch, such as the dorsal root ganglion (*drg*) of an E13 *UBR3*$^{-/-}$ embryo (*A*), the trigeminal ganglion (*TG*) of a P2 *UBR3*$^{-/-}$ pup (*B* and *C*), as well as the upper part (*solid arrowheads*) and superficial end of vibrissal follicle-sinus complexes of a P1 *UBR3*$^{-/-}$ pup (*D–F*). *nt*, neural tube; *nc*, nasal cavity; *tn*, tongue; *sn*, sinus; *hs*, hair shaft; *hf*, hair follicle; *m*, matrix. *G–J*, expression of *UBR3* in auditory and balancing organs, particularly in the spiral ganglion (*SG*) and the OC of the cochlea in the inner ear (*G–I*). Inner hair cells (*IHC*) and outer hair cells (*OHC*) in the organ of Corti that express *UBR3* (*I*) are mechanosensory cells. *UBR3* is also expressed in the sensory epithelium of macula (*J*) and the vestibular ganglion (*VG*) (*G*) of the balancing system. *GG*, geniculate ganglion. *K* and *L*, expression of *UBR3* in the organs of taste, especially in taste buds of three papillae (fungiform (*fgp*), foliate (*flp*), and circumvallate papillae (*cvp*)). Note high *UBR3* expression in the sensory epithelium of taste buds (*dashed lines*) (*L*). *M* and *N*, expression of *UBR3* in specific tissues of the eye in a P2 *UBR3*$^{-/-}$ pup, especially in the lens (*Ln*), in the ganglion cell layer (*gcl*) of retina, and in the outer region of developing retina (*arrowhead*).

behavior. *UBR3* was found to be prominently expressed in taste buds of the fungiform, circumvallate, and foliate papillae, where ~50–100 taste sensory cells are organized into anatomically distinct groups (Fig. 6, *K* and *L*). Auditory information (the intensity and frequencies of sound) is received and relayed by mechanosensory hair cells in the organ of Corti of the inner ear. Voltage-gated channels in the stereocilia of hair cells open and close in response to physical movements of hairs (specialized cilia), giving rise to action potentials (57). Hair cells form synapses with cells of the innervated spiral (cochlear) ganglion, thereby relaying their signals to specific regions of the brain. *UBR3* was prominently expressed, in spatially confined patterns, in the spiral ganglion and the organ of Corti of the cochlea in the inner ear (Fig. 6, *G–I*). In the organ of Corti, *UBR3* was expressed in the inner hair cells and outer hair cells, both of which are mechanosensory cells. *UBR3*-specific LacZ staining was also present in the sensory epithelium of macula and vestibular ganglion of the balancing system (Fig. 6, *G* and *J*). Photons of light are detected by photoreceptor cells in the retina and are transduced into action potentials by light-activated cells. These signals, transmitted and processed by bipolar neurons and the rest of the retinal neural network, are conveyed via the optic nerve to specific regions of the brain (58, 59). Similarly to the findings with other sensory organs (Figs. 5 and 6, *A–L*), the expression of *LacZ/UBR3* was conspicuous in the ganglion cell layer and developing photoreceptor cells of the retina (Fig. 6, *M* and *N*). In summary, the *UBR*-specific LacZ marker was specifically and prominently expressed in sensory cells that underlie the major five senses (smell, touch, vision, hearing, and taste), suggesting that UBR3-dependent ubiquitylation regulates the reception or processing of sensory signals (Figs. 5 and 6).

Expression of LacZ/UBR3 in Sensory Cells for Taste, Hearing, and Vision—Chemosensation includes smell and taste. Taste receptor cells respond to gustatory stimuli through GPCRs and ion channels (55, 56). When stimulated, these cells produce action potentials that relay gustatory signals to relevant regions of the brain. Since gustatory sensation provides information about the quantity and quality of food, including whether it should be swallowed, the sensing of taste may affect suckling

Because *UBR3* is also expressed outside the nervous system (Fig. 1*D*), its remarkably specific expression patterns in sensory tissues (Figs. 5 and 6) reflect only a subset of UBR3 functions, most of which remain to be discovered. In this initial study of

TABLE 2
Measurements of neurotransmitters and related compounds in *UBR3*$^{-/-}$ mice
Data represent mean values ± S.E.

	Noradrenaline	Dopamine	Homovanillic acid	γ-Aminobutyric acid	Glutamate	Serotonin	5-Hydroxyindoleacetic acid	Taurine	Tyrosine
	pg/mg tissue	*pg/mg tissue*	*pg/mg tissue*	*pmol/mg tissue*	*pmol/mg tissue*	*pg/mg tissue*	*pg/mg tissue*	*pmol/mg tissue*	*pmol/mg tissue*
E18 brain[a]									
+/+	95.2 ± 9.7	46.4 ± 7.6	33.1 ± 6.0	1.57 ± 0.06	5.08 ± 0.12	53.9 ± 7.0	217 ± 25	21.6 ± 0.4	3.98 ± 0.29
+/−	85.1 ± 4.2	40.5 ± 4.4	26.7 ± 2.3	1.61 ± 0.04	5.05 ± 0.13	52.7 ± 6.6	209 ± 6	21.1 ± 0.5	3.18 ± 0.19
−/−	89.0 ± 6.7	43.1 ± 4.9	30.4 ± 2.9	1.58 ± 0.06	5.14 ± 0.23	61.7 ± 6.8	183 ± 10	21.7 ± 0.7	3.68 ± 0.20
P1 brain[b]									
+/+	164 ± 9	99.0 ± 3.5	47.3 ± 6.0	1.46 ± 0.09	3.46 ± 0.13	203 ± 33	944 ± 95	27.9 ± 0.9	3.62 ± 0.52
+/−	185 ± 11	108 ± 4.3	41.0 ± 6.4	1.56 ± 0.10	3.77 ± 0.28	245 ± 33	947 ± 89	29.8 ± 1.6	3.68 ± 0.33
−/−	162 ± 3	93.1 ± 2.9	36.3 ± 4.7	1.31 ± 0.04	3.22 ± 0.12	223 ± 46	1114 ± 99	26.7 ± 0.7	3.10 ± 0.26
P1 OB[b]									
+/+	100 ± 16.9	54.9 ± 11.4	55.9 ± 12.3	1.23 ± 0.24	5.14 ± 0.50	61.0 ± 7.2	267 ± 30	38.3 ± 2.4	3.55 ± 0.45
+/−	80.5 ± 19.4	56.8 ± 5.9	51.8 ± 6.2	1.17 ± 0.10	4.43 ± 0.37	66.9 ± 4.0	286 ± 25	31.9 ± 2.5	3.25 ± 0.41
−/−	**41.4 ± 14.3**[c]	32.4 ± 8.6	50.2 ± 12.3	1.00 ± 0.11	3.78 ± 0.38	61.3 ± 9.0	321 ± 40	30.4 ± 2.7	2.62 ± 0.46

[a] +/+ ($n = 7$), +/− ($n = 10$), −/− ($n = 10$).
[b] +/+ ($n = 6$), +/− ($n = 10$), −/− ($n = 7$).
[c] $p < 0.05$ *versus* P1 OB +/+; one-way analysis of variance.

UBR3, which includes its cloning, biochemical characterization, and the construction of *UBR3*$^{-/-}$ mice, we focused on the expression of *UBR3* in sensory organs primarily because of the serendipitous discovery of suckling impairment in *UBR3*$^{-/-}$ neonates (Fig. 4), a defect that is likely to stem, at least in part, from abnormal olfaction.

UBR3$^{-/-}$ *Mice Are Impaired in Olfaction-based Behavior*—Histological examination of sections of B6-enriched *UBR3*$^{-/-}$ heads at E18 or P1 did not detect anatomical abnormalities in OE, OB, and piriform cortex, where *UBR3* is prominently expressed (see above). Immunohistochemical staining of sections from +/+ and *UBR3*$^{-/-}$ P2 pups also did not reveal significant alteration in the expression and distribution of olfactory neuronal markers, such as the olfactory marker protein (*OMP*) and type III adenylyl cyclase (Fig. 5, *H–K*). To determine the survival and growth of neurons, we measured the levels of neurotrophins in *UBR3*$^{-/-}$ animals at E18 and P1 together with littermate controls. *UBR3* knock-out did not affect significantly the levels of nerve growth factor (0.16 ± 0.02 pg/mg of tissue in +/+ ($n = 6$), 0.19 ± 0.02 in +/− ($n = 10$), and 0.15 ± 0.02 in −/− ($n = 7$)) and brain-derived neurotrophic factor (10.1 ± 1.3 pg/mg in +/+ ($n = 6$), 10.5 ± 1.3 in +/− ($n = 10$), and 10.5 ± 0.8 in −/− ($n = 7$)) in the brains of P1 pups, as were E18 embryos (data not shown). Microarray analyses of 22,000 mouse genes (Affymetrix GeneChips) coupled with selective quantitative reverse transcription-PCR with mRNAs isolated from +/+ and *UBR3*$^{-/-}$ P1 brains did not detect genes whose expression was altered more than 2-fold in the mutant.[3]

The ability of olfactory neurons to convey signals to OB is underlain by the biosynthesis, transport, and release of specific neurotransmitters, such as catecholamines (60). We determined the effect of UBR3 loss on the levels of neurotransmitters and related substances, including dopamine, noradrenaline, homovanillic acid (a major catabolite of dopamine), γ-aminobutyric acid, glutamate, serotonin, 5-hydroxyindoleacetic acid, taurine, and tyrosine. In the whole brains at E18 or P1, the absence of UBR3 did not affect the levels of these compounds. In contrast, the OB of P1 *UBR3*$^{-/-}$ neonates contained a significantly reduced level of noradrenaline but not of other tested compounds, compared with control neonates. Dopamine, a precursor of noradrenaline, was also affected in P1 *UBR3*$^{-/-}$ pups to a lesser extent (Table 2). Since earlier studies implicated catecholamines in olfaction and other senses (61–63), the above results (Table 2) suggest that UBR3 is required, in particular, for normal regulation of catecholamines.

The lethality associated with impaired suckling in *UBR3*$^{-/-}$ neonates (Fig. 4) and the expression of *UBR3* in sensory cells of the olfactory pathway (Fig. 5) suggest that one physiological function of UBR3 is in olfaction. To begin addressing this possibility, we employed an odor-based behavioral test, with 7–17-week-old *UBR3*$^{-/-}$ mice that naturally survived or were rescued by litter size reduction. In a pretest, mice were exposed three times (2-min exposures with 1-min intervals) to a water-dipped cotton swab, and the number of times a mouse sniffed or approached to explore the swab was recorded at each trial. The control (+/+ and *UBR3*$^{+/-}$) and the *UBR3*$^{-/-}$ mice (both males and females) proactively sniffed or explored water-dipped swabs in pretests in which swab was a novel object (Fig. 7*A*). The sniffing counts of all three genotypes decreased in subsequent trials in which a water-dipped swab was no longer a novel object (Fig. 7*A*). These results suggest that *UBR3*$^{-/-}$ mice are not significantly impaired in the exploratory activity and are normally habituated to the swab. One minute after the pretest, the same procedure was repeated but with a swab laced with an odorant, such as isoamyl acetate (a pearlike odor), citral (a lemon-like odor), ethyl vanillin (a vanilla-like odor), and geraniol (a rose-like odor). As expected, the control (+/+ and *UBR3*$^{+/-}$) mice actively responded to the swab laced with these odors (Fig. 7*B*). In contrast, *UBR3*$^{-/-}$ mice were found to exhibit the behavioral anosmia toward tested odors. Remarkably, this defect was confined to *UBR3*$^{-/-}$ females (Fig. 7*B*). Thus, UBR3 appears to regulate olfactory behavior and does so, in adult mice, in a gender-specific manner. Together with the expression patterns of *UBR3* (Figs. 1*D*, 5, and 6), these initial functional insights, the beginning of broader explorations, hint at wide ranging functions of UBR3, both inside and outside the nervous system.

[3] T. Tasaki and Y. T. Kwon, unpublished data.

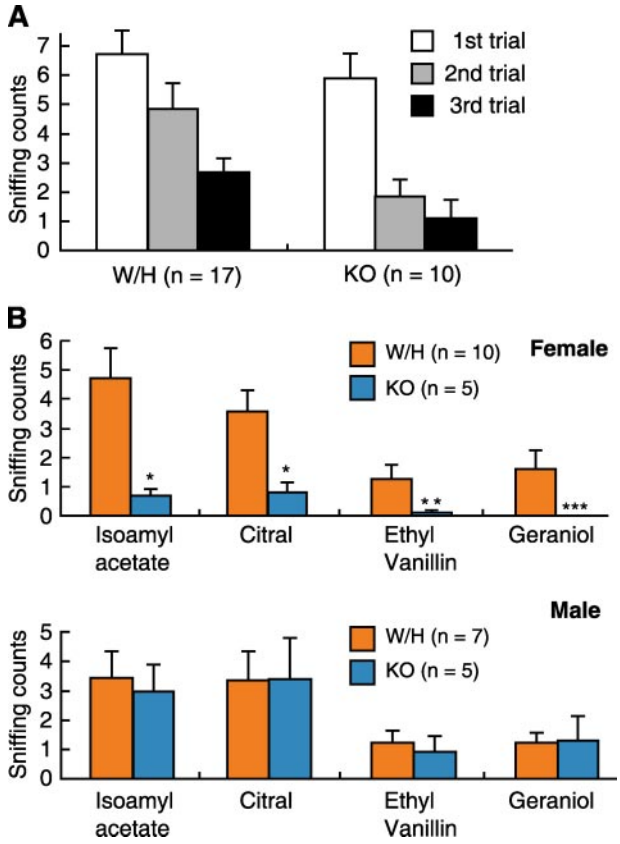

FIGURE 7. **Olfaction-dependent behavioral tests of *UBR3*$^{-/-}$ mice.** *A*, pretesting sessions with +/+ and *UBR3*$^{+/-}$ (wild-type/heterozygous (*W/H*)) *versus UBR3*$^{-/-}$ (*KO*) mice, using a cotton swab laced with water (see "Odor-based Behavioral Tests"; 7–17-week-old mice, with littermates as controls). *B*, control and *UBR3*$^{-/-}$ mice were subjected to four consecutive odorant tests 1 min after pretesting, using isoamyl acetate, citral, ethyl vanillin, and geraniol as odorants. The data are expressed as the S.E. of the sniffing counts during the first 2-min exposures to water or odorants. *, $p < 0.01$; **, $p = 0.06$; ***, the sniffing count was zero. *p* refers to probability values in Welch's *t* test.

DISCUSSION

Our previous work (17) identified mammalian E3 Ub ligases, termed UBR1–UBR7, that contain a distinct domain named the UBR box (Fig. 1, *B* and *C*). These E3s include UBR1 and UBR2, the previously known Ub ligases of the N-end rule pathway. Such E3s recognize N-end rule substrates through the binding, in part through their UBR domains, to destabilizing N-terminal residues. The present study, a part of our ongoing exploration of the UBR family E3s and the N-end rule pathway, describes the cloning and extensive characterization of the mouse UBR3 Ub ligase. We report that UBR3 is a 213-kDa RING finger E3 that also contains the UBR domain and exhibits a low but statistically significant similarity to UBR1 and UBR2 outside the above two domains as well. (The sequence of UBR3 is 22% identical to those of UBR1 and UBR2, which are 47% identical.) These three Ub ligases are, thus far, the sole members of the RING-UBR subfamily of the above UBR family of E3s. We found that UBR3 interacts with the Ub-conjugating (E2) enzymes HR6A or HR6B, which also interact with the other two E3s of the RING-UBR subfamily, the UBR1 and UBR2 Ub ligases of the N-end rule pathway. Despite this similarity and the presence of a UBR box in UBR3, our findings indicate that UBR3 does not bind to known N-end rule substrates of UBR1 and UBR2.

The fact that only a subset of UBR-box proteins can bind to destabilizing N-terminal residues (16, 17) (this study), indicates that the sequence motif termed the UBR box (Fig. 1*C*) functions as a scaffold for specific three-dimensional structures of distinct binding specificities. At present, the only known class of specific ligands that bind to UBR boxes is that of N-degrons, specifically their destabilizing N-terminal residues, in either protein size or peptide size ligands. However, given our results with UBR3 (Fig. 2), other, non-N-end rule physiological ligands of the UBR domain (*e.g.* those that bind to UBR of UBR3) are expected to exist as well. One function of the UBR boxes in the known N-recognins (Fig. 1) is nutritional sensing. Specifically, *S. cerevisiae* UBR1 binds, in part through its UBR box, to short peptides bearing destabilizing N-terminal residues. This binding allosterically activates a third substrate-binding site of UBR1 that targets an internal (non-N-degron) degradation signal of CUP9, a transcriptional repressor of peptide import. This design of yeast UBR1 yields a positive feedback circuit that can detect intracellular peptides and up-regulate their import (16, 26, 33). By analogy, a UBR box of UBR3 may bind to (currently unknown) small metabolites. Similarly to the binding of dipeptides to the type-1/2 binding sites of UBR1 (see Introduction), the binding of a small effector to UBR3 may activate its other substrate-binding site (presumed to exist by analogy to UBR1/UBR2), thereby altering the rate of ubiquitylation of a relevant regulatory protein(s). If so, one interesting possibility is that a small compound ligand and/or a protein target(s) of UBR3 may be the same in otherwise diverse physiological processes that involve UBR3 in different sensory tissues.

The phenotypes of *UBR3*$^{-/-}$ mouse strains that were characterized in this work are strongly dependent on genetic background. Specifically, *UBR3*$^{-/-}$ mice of the inbred (129S) background died as early embryos, for reasons that remain to be determined. In contrast, *UBR3*$^{-/-}$ mice of the mixed (B6/129S) background, although they were born at lower than expected frequencies (Table 1), were fertile, of normal size, and apparently normal otherwise as well. Remarkably, our systematic, long term (over ~3 years) enrichment of *UBR3*$^{-/-}$ mice in the B6 genetic background yielded a reproducible and conspicuous phenotype, a strongly increased lethality of newborn *UBR3*$^{-/-}$ pups, largely if not entirely because of impaired suckling (Fig. 4 and Table 1). The dependence of viability and other phenotypes of *UBR3*$^{-/-}$ mice on their genetic background (Table 1) indicate the presence of genes whose alleles functionally interact with *UBR3*.

The finding that UBR3 is prominently expressed in neurons and/or other cells that mediate sensory pathways, including the five major senses (Figs. 5 and 6), suggested a role of UBR3 in the corresponding physiological processes. The vision, smell, and taste are mediated primarily by specific GPCR signaling pathways. For example, the rhodopsin, a photon-stimulated photoreceptor in the eye's retina, initiates a cGMP-dependent signal transduction cascade that leads to the action potential (58). The MOE, the VNO, and taste buds also express specific GPCRs that recognize, respectively, various odorants, pheromones, and a set of substances that elicit sensations of taste, such as *sweet*, *bitter*, and *umami* (56). The second messengers for these sensory GPCR signaling pathways are primarily cyclic AMP (olfactory neurons and taste sensory cells (for *sweet* and

umami)) and inositol 1,4,5-trisphosphate (vomeronasal sensory neuron and taste sensory cells (for *bitter*)), in contrast to cGMP in photoreceptor cells. The taste sensory cells utilize sodium and potassium channels to sense, respectively, *salty* and *sour* substances, and the signal transduction cascades involved do not depend on GPCR activation. In yet another example of the diversity of signaling pathways in different sensory organs, the senses of touch and hearing are triggered by mechanical force-transducing molecules, such as mechanosensitive ion channels. In sum, the mechanisms underlying signal reception, receptor activation, and intracellular signal transduction tend to be distinct in different sensory settings. By contrast, the processes of synaptic transmission, downstream of the above signaling cascades, involve largely similar molecular mechanisms. Thus, one possibility is that UBR3, which is expressed in all of the above sensory systems (in addition to other cell types as well), may regulate a common step of "downstream" synaptic transmission rather than signal initiation or intracellular signal transduction. Reduced amounts of noradrenaline and dopamine in olfactory bulbs of *UBR3*$^{-/-}$ pups (Table 2) are consistent with this possibility.

Because a suckling defect of *UBR3*$^{-/-}$ pups, which could be partially rescued by a decreased litter size, can be caused by impaired olfaction, and because UBR3 is expressed in olfactory tissues (Fig. 5; see "Results"), we carried out tests for behavioral anosmia in *UBR3*$^{-/-}$ mice. Strikingly, the anosmia in adult *UBR3*$^{-/-}$ mice, although present and strong, was found to be confined to *UBR3*$^{-/-}$ females, whereas the increased lethality of *UBR3*$^{-/-}$ neonates in the B6-enriched background was gender-neutral (Table 1). This gender-specific difference in olfactory behavior (Table 1 and Fig. 7) can be reconciled if newly born *UBR3*$^{-/-}$ pups of either gender were anosmic and if *UBR3*$^{-/-}$ males but not *UBR3*$^{-/-}$ females recovered their olfaction by the time of sexual maturity, when behavioral tests for anosmia were carried out. Examination of these and related possibilities will require electrophysiological tests with nasal epithelia of wild-type and mutant pups. To the best of our knowledge, a gender dependence of anosmia has been reported in regard to the induction of olfactory sensitivity in normal humans (64) but not in a mouse mutant (Fig. 7). One possibility is that a suppressor gene in the male-specific Y chromosome rescues the anosmia phenotype of adult *UBR3*$^{-/-}$ males. A putative Y-borne suppressor may or may not be a Ub ligase.

Since *UBR3* is also expressed outside the nervous system (Fig. 1*D*), its remarkably specific expression patterns in sensory tissues (Figs. 5 and 6) reflect only a subset of UBR3 functions, most of which remain to be discovered. Our initial functional results (Fig. 7), the beginning of broader explorations, hint at wide-ranging roles of UBR3, both inside and outside the nervous system.

Acknowledgments—We are grateful to Jai Wha Seo for genotyping and maintaining mouse strains, to S. Pease (Caltech) for assistance with ES cell work, to B. Kennedy (Caltech) and the staff of the animal facility at the University of Pittsburgh for the care and maintenance of mice, and to A. Arnswald and A. Bunge for excellent technical assistance.

REFERENCES

1. Fang, S., and Weissman, A. M. (2004) *Cell Mol. Life. Sci.* **61,** 1546–1561
2. Hochstrasser, M. (2006) *Cell* **124,** 27–34
3. Petroski, M. D., and Deshaies, R. J. (2005) *Nat. Rev. Mol. Cell. Biol.* **6,** 9–20
4. Varshavsky, A. (2006) *Pro. Sci.* **15,** 647–654
5. Bachmair, A., and Varshavsky, A. (1989) *Cell* **56,** 1019–1032
6. Gardner, R. G., and Hampton, R. Y. (1999) *EMBO J.* **18,** 5994–6004
7. Suzuki, T., and Varshavsky, A. (1999) *EMBO J.* **18,** 6017–6026
8. Sheng, J., Kumagai, A., Dunphy, W. G., and Varshavsky, A. (2002) *EMBO J.* **21,** 6061–6071
9. Cardozo, T., and Pagano, M. (2004) *Nat. Rev. Mol. Cell. Biol.* **5,** 739–751
10. Ardley, H. C., and Robinson, P. A. (2005) *Essays Biochem.* **41,** 15–30
11. Baumeister, W., Walz, J., Zühl, F., and Seemüller, E. (1998) *Cell* **92,** 367–380
12. Finley, D., Bartel, B., and Varshavsky, A. (1989) *Nature* **338,** 394–401
13. Schnell, J. D., and Hicke, L. (2003) *J. Biol. Chem.* **278,** 35857–35860
14. Bachmair, A., Finley, D., and Varshavsky, A. (1986) *Science* **234,** 179–186
15. Varshavsky, A. (1996) *Proc. Natl. Acad. Sci. U. S. A.* **93,** 12142–12149
16. Kwon, Y. T., Xia, Z. X., An, J. Y., Tasaki, T., Davydov, I. V., Seo, J. W., Xie, Y., and Varshavsky, A. (2003) *Mol. Cell. Biol.* **23,** 8255–8271
17. Tasaki, T., Mulder, L. C. F., Iwamatsu, A., Lee, M. J., Davydov, I. V., Varshavsky, A., Muesing, M., and Kwon, Y. T. (2005) *Mol. Cell. Biol.* **25,** 7120–7136
18. Hu, R.-G., Sheng, J., Xin, Q., Xu, Z., Takahashi, T. T., and Varshavsky, A. (2005) *Nature* **437,** 981–986
19. Hu, R.-G., Brower, C. S., Wang, H., Davydov, I. V., Sheng, J., Zhou, J., Kwon, Y. T., and Varshavsky, A. (2006) *J. Biol. Chem.* **281,** 32559–32573
20. Johnson, E. S., Gonda, D. K., and Varshavsky, A. (1990) *Nature* **346,** 287–291
21. Prakash, S., Tian, L., Ratliff, K. S., Lehotzky, R. E., and Matouschek, A. (2004) *Nat. Struct. Mol. Biol.* **11,** 830–837
22. Kwon, Y. T., Balogh, S. A., Davydov, I. V., Kashina, A. S., Yoon, J. K., Xie, Y., Gaur, A., Hyde, L., Denenberg, V. H., and Varshavsky, A. (2000) *Mol. Cell. Biol.* **20,** 4135–4148
23. Kwon, Y. T., Kashina, A. S., and Varshavsky, A. (1999) *Mol. Cell. Biol.* **19,** 182–193
24. Kwon, Y. T., Kashina, A. S., Davydov, I. V., Hu, R.-G., An, J. Y., Seo, J. W., Du, F., and Varshavsky, A. (2002) *Science* **297,** 96–99
25. Lee, M. J., Tasaki, T., Moroi, K., An, J. Y., Kimura, S., Davydov, I. V., and Kwon, Y. T. (2005) *Proc. Natl. Acad. Sci. U. S. A.* **102,** 15030–15035
26. Turner, G. C., Du, F., and Varshavsky, A. (2000) *Nature* **405,** 579–583
27. Rao, H., Uhlmann, F., Nasmyth, K., and Varshavsky, A. (2001) *Nature* **410,** 955–960
28. Ditzel, M., Wilson, R., Tenev, T., Zachariou, A., Paul, A., Deas, E., and Meier, P. (2003) *Nat. Cell Biol.* **5,** 467–473
29. Varshavsky, A. (2003) *Nat. Cell Biol.* **5,** 373–376
30. Yoshida, S., Ito, M., Gallis, J., Nishida, I., and Watanabe, A. (2002) *Plant J.* **32,** 129–137
31. An, J. Y., Seo, J. W., Tasaki, T., Lee, M. J., Varshavsky, A., and Kwon, Y. T. (2006) *Proc. Natl. Acad. Sci. U. S. A.* **103,** 6212–6217
32. Zenker, M., Mayerle, J., Lerch, M. M., Tagariello, A., Zerres, K., Durie, P. R., Beier, M., Hülskamp, G., Guzman, C., Rehder, H., Beemer, F. A., Hamel, B., Vanlieferinghen, P., Gershoni-Baruch, R., Vieira, M. W., Dumic, M., Auslender, R., Gil-da-Silva-Lopes, V. L., Steinlicht, S., Rauh, R., Shalev, S. A., Thiel, C., Winterpacht, A., Kwon, Y. T., Varshavsky, A., and Reis, A. (2005) *Nat. Genet.* **37,** 1345–1350
33. Du, F., Navarro-Garcia, F., Xia, Z., Tasaki, T., and Varshavsky, A. (2002) *Proc. Natl. Acad. Sci. U. S. A.* **99,** 14110–14115
34. Kwon, Y. T., Xia, Z., Davydov, I. V., Lecker, S. H., and Varshavsky, A. (2001) *Mol. Cell. Biol.* **21,** 8007–8021
35. Erbse, A., Schmidt, R., Bornemann, T., Schneider-Mergener, J., Mogk, A., Zahn, R., Dougan, D. A., and Bukau, B. (2005) *Nature* **439,** 753–756
36. Kwon, Y. T., Reiss, Y., Fried, V. A., Hershko, A., Yoon, J. K., Gonda, D. K., Sangan, P., Copeland, N. G., Jenkins, N. A., and Varshavsky, A. (1998) *Proc. Natl. Acad. Sci. U. S. A.* **95,** 7898–7903
37. Sasaki, T., Kojima, H., Kishimoto, R., Ikeda, A., Kunimoto, H., and Nakajima, K. (2006) *Mol. Cell* **24,** 63–75

38. Ausubel, F. M., Brent, R., Kingston, R. E., Moore, D. D., Smith, J. A., Seidman, J. G., and Struhl, K. (eds). (2002) *Current Protocols in Molecular Biology*, Wiley-Interscience, New York
39. Harlow, E., and Lane, D. (1999) Using Antibodies: a laboratory manual, Cold Spring Harbor Laboratory Press, Cold Spring Harbor, NY
40. Chourbaji, S., Hellweg, R., Brandis, D., Zörner, B., Zacher, C., Lang, U. E., Henn, F. A., Hörtnagl, H., and Gass, P. (2004) *Brain Res. Mol. Brain Res.* **121,** 28–36
41. Piepponen, T. P., and Skujins, A. (2001) *J. Chromatogr. B. Biomed. Sci. Appl.* **757,** 277–283
42. Hellweg, R., Baethge, C., Hartung, H. D., Bruckner, M. K., and Arendt, T. (1996) *Neuroreport* **7,** 777–780
43. Trinh, K., and Storm, D. R. (2003) *Nat. Neurosci.* **6,** 519–525
44. Dohmen, R. J., Madura, K., Bartel, B., and Varshavsky, A. (1991) *Proc. Natl. Acad. Sci. U. S. A.* **88,** 7351–7355
45. Dover, J. J., Schneider, J., Boateng, M. A., Wood, A., Dean, K., Johnston, M., and Shilatifard, A. (2002) *J. Biol. Chem.* **277,** 28368–28371
46. Wang, L., Mao, X., Ju, D., and Xie, Y. (2004) *J. Biol. Chem.* **279,** 55218–55223
47. Belluscio, L., Gold, G. H., Nemes, A., and Axel, R. (1998) *Neuron* **20,** 69–81
48. Wong, S. T., Trinh, K., Hacker, B., Chan, G. C., Lowe, G., Gaggar, A., Xia, Z., Gold, G. H., and Storm, D. R. (2000) *Neuron* **27,** 487–497
49. Kutsuwada, T., Sakimura, K., Manabe, T., Takayama, C., Katakura, N., Kushiya, E., Natsume, R., Watanabe, M., Inoue, Y., Yagi, T., Aizawa, S., Arakawa, M., Takahashi, T., Nakamura, Y., Mori, H., and Mishina, M. (1996) *Neuron* **16,** 333–344
50. Brunet, L. J., Gold, G. H., and Ngai, J. (1996) *Neuron* **17,** 681–693
51. Mombaerts, P. (2004) *Nat. Rev. Neurosci.* **5,** 263–278
52. Ache, B. A., and Young, J. M. (2005) *Neuron* **48,** 417–430
53. Buck, L., and Axel, R. (1991) *Cell* **65,** 175–187
54. Firestein, S. (2001) *Nature* **413,** 211–218
55. Lindemann, B. (2001) *Nature* **413,** 219–225
56. Scott, K. (2005) *Neuron* **48,** 455–464
57. Lin, S. Y., and Corey, D. P. (2005) *Curr. Opin. Neurobiol.* **15,** 350–357
58. Maeda, T., Imanishi, Y., and Palczewski, K. (2003) *Prog. Retin. Eye Res.* **22,** 417–434
59. Burns, M. E., and Arshavsky, V. Y. (2005) *Neuron* **48,** 387–401
60. Murphy, G. J., Darcy, D. P., and Isaacson, J. S. (2005) *Nat. Neurosci.* **8,** 354–364
61. Bear, M. F., and Singer, W. (1986) *Nature* **320,** 172–176
62. Guan, X., Blank, J., and Dluzen, D. (1993) *Brain Res.* **622,** 51–57
63. Smeets, W. J., and Gonzalez, A. (2000) *Brain Res. Rev.* **33,** 308–379
64. Dalton, P., Doolittle, N., and Breslin, P. A. (2002) *Nat. Neurosci.* **5,** 199–200